

Silicon waveguide-based single cavity Fano resonance temperature sensor*

WANG Shuai, LU Wenda, LAI Xiaohan, WANG Hong, ZHU Lianqing**, and LU Lidan**

Key Laboratory of the Ministry of Education for Optoelectronic Measurement Technology and Instrument, Beijing Information Science and Technology University, Beijing 100059, China

(Received 17 October 2022; Revised 22 November 2022)

©Tianjin University of Technology 2023

A compact Fano resonant temperature sensor composed of a micro-ring resonator (MRR) coupled double-T-shaped waveguide is developed. The coupling gap and coefficient of the device are optimized by the finite difference time domain (FDTD) method. The maximum slope ratio (SR) of the MRR-coupled single-T-shaped waveguide is -2.13 dB/nm. The SR of the double-T-shaped waveguide is -49.69 dB/nm which is 23 times that of the single-T-shaped waveguide. The simulation results show that the temperature sensitivity of optical intensity decreases with increasing temperature in the range from 303.6 K to 343.8 K. The wavelength-temperature sensitivity of the double-T-shaped waveguide microring is 76.5 pm/K. After introducing the double-T-shaped waveguide structure, the device's performance is greatly improved, and the double-T-shaped waveguide has a good application prospect as a temperature sensor.

Document code: A **Article ID:** 1673-1905(2023)03-0139-5

DOI <https://doi.org/10.1007/s11801-023-2177-z>

In recent years, sensor performance has been dramatically improved in high precision, high sensitivity, compactness, and integration. Accurate temperature detection and control are essential in scientific research and production practice. Silicon photonics-based optoelectronic sensors have many advantages, such as high sensitivity, small size, low loss, effortless control, and low cost. For miniaturization and integration of micro-ring resonator (MRR), it has been widely developed in the military^[1], environmental monitoring^[2], medical^[3], and food safety^[4].

Fano resonance is a resonance scattering phenomenon. A significant feature is its asymmetric linearity, which has a higher quality factor and a steeper slope than the Lorentzian resonance. CHANG et al^[5] theoretically and experimentally investigated a high-sensitivity Fano resonant temperature sensing method integrating a silicon Bragg reflector, consisting of an air-cladding silicon rib waveguide and a periodic array of holes that allow under etching for field confinement and formation of the Bragg periodicity. ZHU et al^[6] proposed a compact Fano resonant temperature consisting of two metal-insulator-metal (MIM) waveguides and side-coupled polydimethylsiloxane (PDMS) sealed semi-square ring resonator sensor. The wavelength-temperature sensitivity of the sensor is -4 nm/°C. CHAUHAN et al^[7] calculated a plasmonic MIM waveguide sensor with a radius of

0.44 μm , consisting of the main waveguide gap Fabry-Perot structure and a microring resonance coupled to the main waveguide. The sensitivity of the sensor is 1 200 nm/RIU. However, metal-based waveguides have large losses. QIU et al^[8] reported a Fano resonance-based temperature sensor fabricated on thin-film lithium niobate (TFLN) photonic crystal, which achieved a temperature sensitivity of 0.77 nm/°C. ZHANG et al^[9] proposed a plasmonic waveguide coupled with rectangular and two parallel ring resonators for refractive index sensors. However, the size of the above two structures is large. GU et al^[10] proposed that a phase mutation can be generated by inserting an air hole in the bus waveguide, which can be coupled with the microring with a discrete propagation mode to produce Fano resonance. However, its phase factor is small, the spectral resolution is not significantly enhanced, and the structure cannot be realized by the standard 180 nm multi-project wafer process.

Based on the above research, to realize a compact intensity temperature sensor, this paper proposes a structure of runway MRR coupled with double-T-shaped waveguides for generating Fano resonance. Our group^[11] has verified that the Fabry-Perot cavity formed by a T-shaped waveguide can change the phase. However, the spectrum revolution is limited. Thus, a large phase factor should be introduced. Here, double-T-shaped waveguides coupled with MRR can enhance the phase factor. The

* This work has been supported by the National Natural Science Foundation of China (No.62205029), and the State Grid Zhejiang Electric Power Corporation Information & Telecommunication Branch (No.B311XT21004G).

** E-mails: zhulianqing2020@126.com; lldan_dido@bistu.edu.cn

structure proposed in this paper has the advantages of high integration and compactness. Moreover, it can be realized by a standard 180 nm multi-project wafer process. It has excellent potential to expand and improve the performance of MRR-based on-chip devices, such as sensors, optical switches, and filters. A compact and stable device that exhibits a Fano line shape in all resonant modes is presented and simulated using the finite difference time domain (FDTD) solutions (Lumerical inc.). A noticeable Fano-like spectrum was obtained by optimizing the T-shaped structure's coupling coefficient, phase, and coupling gap. Then, the optical intensity-temperature sensitivity and wavelength-temperature sensitivity of the device are simulated.

The Fano resonance phenomenon of silicon-based photonic devices is usually analyzed by coupled-mode theory (CMT)^[12] or the transfer matrix method (TTM). The influence of the coupling coefficient and the intrinsic parameters of the coupled cavity was analyzed by CMT. The TTM is the analysis method for silicon photonics devices. The complex device structure can be disassembled into fundamental silicon photonics components, each fundamental component has its transmission matrix, and the output spectrum of the device can be obtained by matrix multiplication. Therefore, to intuitively analyze the structure parameters, this paper uses the TTM to analyze the MRR-coupled double-T-shaped waveguide structure. The structure of MRR is shown in Fig.1(a). The input light will be divided into two parts when it propagates to the coupling region, and the last two parts of light will be superimposed by interference at the output port. When the incident optical field propagates in the bus waveguide with $E_{in}=E_0$, the output electrical E_{out} in the bus waveguide MRR structure can be expressed by^[10]

$$E_{out} = tE_0 + i\kappa E_1 + i\kappa E_2 + \dots = \left(t - \frac{\kappa^2 \alpha e^{i\delta}}{1 - t\alpha e^{i\delta}} \right) E_0, \quad (1)$$

where t and κ_1 (κ_2) are the coupling region's transmission coefficient and coupling coefficient, respectively. α is the linear loss coefficient, and E_1 and E_2 represent the electric fields from incident light that runs through one circle and two circles in the MRR. The continuous state light is transmitted in the bus waveguide, representing with tE_0 . The optical field is $E_1=i\kappa\alpha E_0 e^{i\delta}$ when the light propagates one circle in the microring resonator and returns to the coupling region, where δ is the round-trip phase shift, and $\delta=2\pi nL_R/\lambda$, n represents the effective refractive index of the waveguide section. λ is the working wavelength, and L_R is the perimeter of the microring resonator.

The structure of the Fano resonant device designed is shown in Fig.1(c), consisting of two T-shaped waveguides coupled by microring. The device is based on a standard silicon-on-insulator (SOI) with a top layer silicon thickness of 220 nm and a buried silicon oxide layer of 2 μm . The waveguide width is 450 nm, leading to a fundamental mode (TE₀) in the waveguide. The ra-

dius R of the runway microring is set to 10 μm to achieve low bending loss transmission. When incident light passes through one T-shaped waveguide, the continuous propagating mode on the microring introduces a phase $\Delta\Phi$. Thus, tE_0 becomes $te^{-2i\Delta\Phi}E_0$ for two T-shaped waveguides. Without changing the microring structure, the optical field in the discrete state does not introduce phase shift. Therefore, the output field of MRR coupled with a double-T-shaped waveguide is

$$E_{out} = \left(te^{-2i\Delta\Phi} - \frac{\kappa_1 \kappa_2 \alpha e^{i\delta}}{1 - t\alpha e^{i\delta}} \right) E_0. \quad (2)$$

The final transmission spectrum is

$$T(\lambda) = \left| \frac{E_{out}}{E_{in}} \right|^2 = \left| te^{-2i\Delta\Phi} - \frac{\kappa_1 \kappa_2 \alpha e^{i2\pi nL_R/\lambda}}{1 - t\alpha e^{i2\pi nL_R/\lambda}} \right|^2. \quad (3)$$

With the proposed device, it can be used for temperature measurement. Temperature sensing originates from the thermo-optic effect of the silicon material itself. The resonant wavelength change $\Delta\lambda$ caused by temperature change can be expressed as

$$\Delta\lambda = \frac{\lambda \Delta T}{n_g} \left(\frac{\partial n}{\partial T} + \frac{n}{L} \frac{\partial L}{\partial T} \right), \quad (4)$$

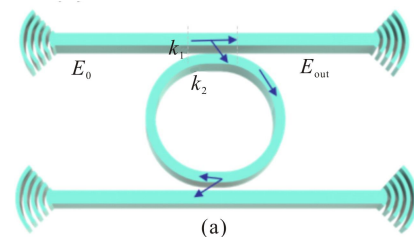
where n_g is the group refractive index of the resonator, and L is the perimeter of the microring.

The temperature sensitivity was improved by taking advantage of the high slope of Fano's linear edges. The optical intensity-temperature sensitivity can be expressed as

$$S_v = k \cdot S_\lambda, \quad (5)$$

where k [dB/nm] is the spectral resolution of the steep Fano edge, and S_v [dB/°C] is the slope-temperature sensitivity. S_λ [pm/°C] is wavelength-temperature sensitivity.

The normalized transmission spectra (NTS) of the runway microring coupled with a single-T-shaped waveguide and a double-T-shaped waveguide are shown in Fig.1(b) according to Eqs.(1) and (3). The Fano line shape of the runway microring coupled with a double-T-shaped waveguide is significantly better than that with a single waveguide. According to the result in the figure, the normalized slope ratio (SR) of the runway microring coupled with a single-T-shaped waveguide is 0.31 nm^{-1} , and the normalized SR of the runway microring coupled with a double-T-shaped waveguide is 0.97 nm^{-1} . It can be seen that the spectral slope of the runway microring coupled with a double-T-shaped waveguide is larger than that of the runway microring coupled with a single-T-shaped waveguide. That is, the spectral resolution is high.



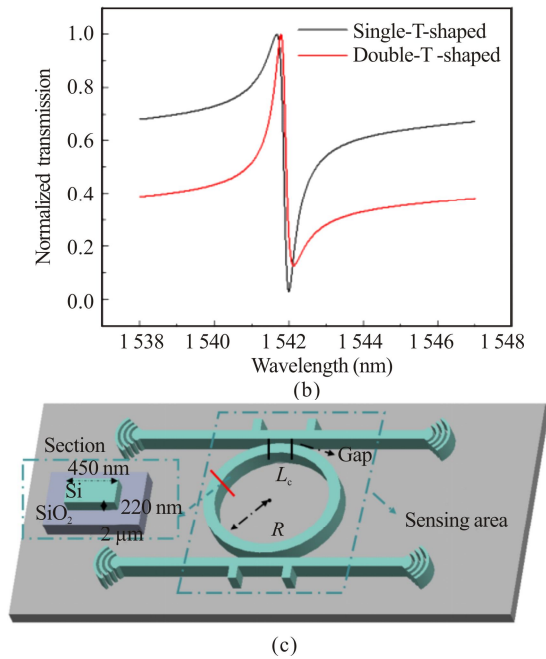


Fig.1 (a) Runway microring device; (b) Normalized transmission spectra of single-T-shaped waveguide and double-T-shaped waveguide microrings; (c) Schematic diagram of runway microring with double-T-shaped waveguide

According to Eq.(3), the relationship between the transmission spectrum and different phases $\Delta\Phi$ is obtained by simulation, where the radius of the runway microring is $R=10\ \mu\text{m}$, the length of the straight waveguide in the runway is $L_c=1\ \mu\text{m}$, $\alpha=0.95$, and the coupling coefficient is $\kappa=0.215$. The figure of merit (*FOM*) is shown in Fig.2(b). *FOM* was characterized by two critical parameters, *ER* and *SR* comprehensively. The relationship of *ER*, *SR*, and *FOM* is $FOM=ER\cdot SR$. *SR*, *ER*, and *FOM* reach their reflection point when $\Delta\Phi=0.248\pi$.

Based on the analysis of $\Delta\Phi$, when $R=10\ \mu\text{m}$, $\alpha=0.95$, $\Delta\Phi=0.248\pi$, the transmission spectra corresponding to different κ values are shown in Fig.2(c). It can be seen that the *ER* is optimal when the coupling coefficient is $\kappa=0.312$. As shown in Fig.2(d), when $\kappa=0.312$, the extinction ratio is at the inflection point. When κ is too small, the coupling coefficient is relatively small. And the coupling distance is too large when the coupling length is constant. On the contrary, when κ is large, the coupling coefficient leads to a small coupling distance, which needs a high processing accuracy.

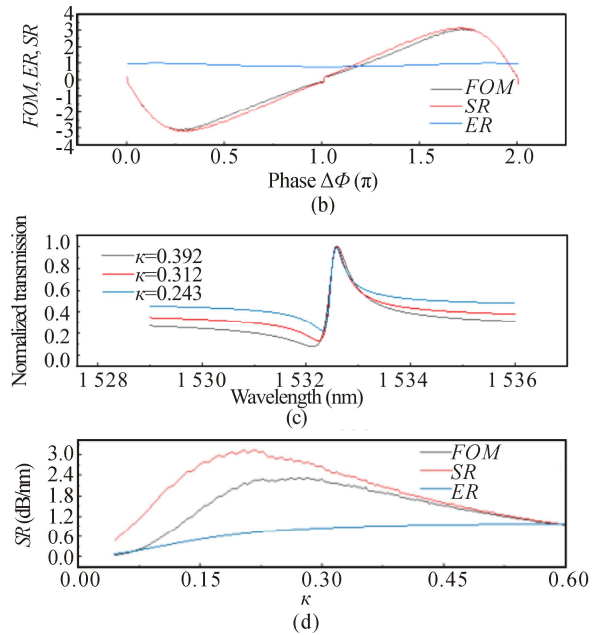
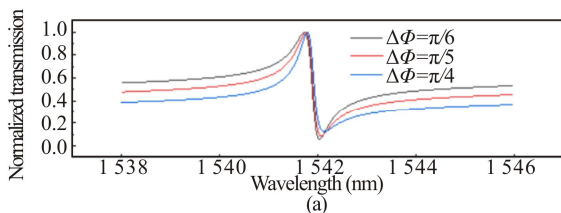


Fig.2 (a) Transmission spectra corresponding to different $\Delta\Phi$ values; (b) *FOM*, *SR*, *ER* curves in the $\Delta\Phi$ range of $0-\pi$; (c) Transmission spectra corresponding to different κ values; (d) *FOM*, *SR*, *ER* curves in the κ range of $0-1$

The device is simulated using the FDTD method to obtain more accurate results. The changes in *ER* and *SR* of the Fano resonance spectrum are observed by adjusting the coupling gap (g) between the microring and the bus waveguide. The simulation uses a broadband optical source in the wavelength range from 1500 nm to 1600 nm. The height of the T-shaped waveguide was fixed at $0.8\ \mu\text{m}$ to verify the effect of the coupling spacing g on the Fano resonance spectrum. The transmission spectra obtained by selecting $g=0.1\ \mu\text{m}$, $0.15\ \mu\text{m}$, $0.2\ \mu\text{m}$, and $0.25\ \mu\text{m}$ are shown in Fig.3. It can be seen that when $g=0.1\ \mu\text{m}$, the transmission spectrum has no Fano resonance line shape. When $g=0.2\ \mu\text{m}$, the *ER* is small. However, when $g=0.15\ \mu\text{m}$, the Fano resonance line shape is the best.

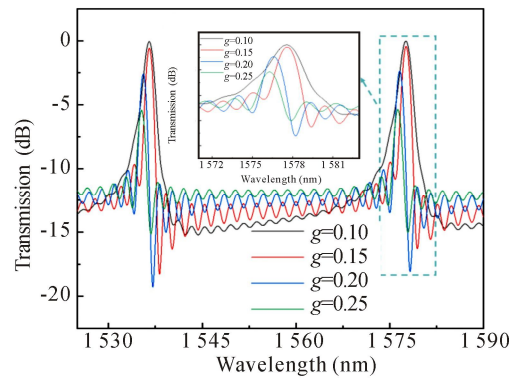


Fig.3 Transmission spectra corresponding to different g values

The effective refractive index in silicon can change by

temperature for the thermo-optic effect. A small temperature variation would change the transmission spectrum of MRR. It has been verified that the Fano resonance devices can obtain high-temperature sensitivity^[13-18]. As shown in Fig.4, the optical intensity-temperature and wavelength-temperature sensitivity are obtained by simulating the change of transmission spectrum with different temperatures through Mode Solution (Ansys. Lumerical. Inc.). The thermo-optic coefficient of silicon is $dn/dT=1.84 \times 10^{-4} \text{ K}^{-1}$. The temperature ranges are 303.6—304.2 K, 313.6—314.2 K, and 343.2—343.8 K, with an increase of 0.1 K.

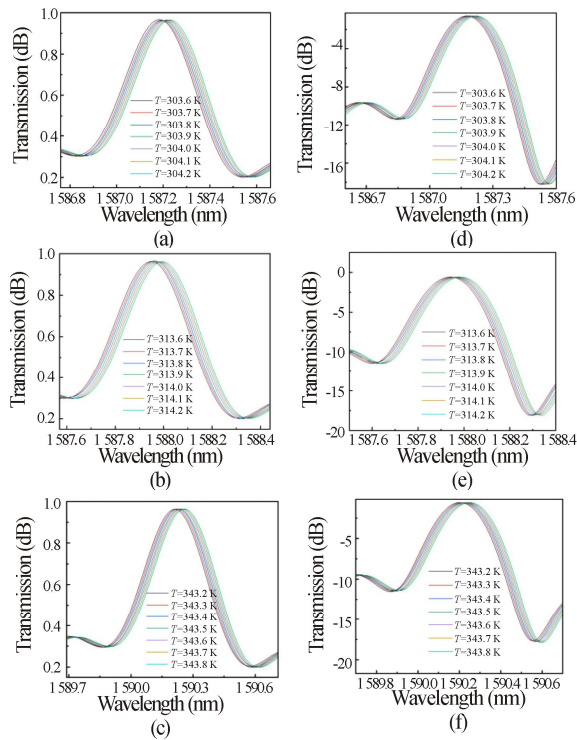


Fig.4 Transmission spectra of single-T-shaped waveguide microring in the temperature ranges of (a) 300.6—301.2 K, (b) 313.6—314.2 K, and (c) 343.2—343.8 K; Transmission spectra of double-T-shaped waveguide microring in the temperature ranges of (d) 300.6—301.2 K, (e) 313.6—314.2 K, and (f) 343.2—343.8 K

The formula process of optical intensity temperature sensitivity can be expressed as follows

$$\frac{dP}{dT} = \frac{dP}{d\lambda} \cdot \frac{d\lambda}{dT} = SR \cdot \frac{d\lambda}{dT}, \quad (6)$$

where dP is the optical intensity, dT is the temperature, and $d\lambda$ is the wavelength. The optical intensity-temperature sensitivities of the single-T-shaped waveguide microring and the double-T-shaped waveguide microring are -0.15 dB/K and -4.07 dB/K , respectively, with the temperature ranging from 303.6 K to 304.2 K. The optical intensity-temperature sensitivities of the single-T-shaped waveguide microring and the double-T-shaped waveguide microring are -0.16 dB/K and -3.83 dB/K , respectively, with temperatures ranging

from 313.6 K to 314.2 K. The optical intensity-temperature sensitivity in the temperature range of 343.2—344.8 K is -0.18 dB/K and -3.79 dB/K , respectively. Tab.1 shows the maximum SR of the single-T-shaped waveguide microring and the double-T-shaped waveguide microring at different temperatures. The wavelength-temperature relationship of the double-T-shaped waveguide microring is shown in Fig.5, with a wavelength-temperature sensitivity of 76.5 pm/K .

Tab.1 SR values at different temperatures

Temperature (K)	Single-T-shaped (dB/nm)	Double-T-shaped (dB/nm)
303.6—304.2	-2.13	-49.69
313.6—314.2	-2.11	-49.67
343.2—343.8	-2.12	-49.03

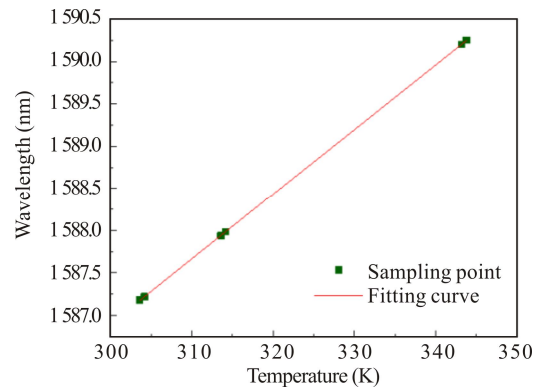


Fig.5 Fitting curve of experimental data showing the wavelength shift as a linear function of temperature

The above analysis concludes that within the appropriate temperature range, the optical intensity-temperature sensitivity would decrease with the increase in temperature. Compared with single-T-shaped waveguide microring, the double-T-shaped waveguide microring has higher SR .

In conclusion, by adding two T-shaped waveguides in the coupling region, we have demonstrated that the resonance peak is a Fano resonance line in the broader band. The spectral resolution of double-T-shaped runway microring is higher than that of single-T-shaped runway microring. The coupling gap g greatly influences ER and SR of the spectrum. When the gap is too small, the spectrum does not show the Fano lineshape. When the gap is too large, the extinction of the Fano device is relatively small. The preliminary study shows that the change in temperature causes the change in refractive index and the shift of Fano resonance wavelength. The optical intensity-temperature sensitivity would decrease with the increase in temperature. Overall, this device has great potentials in future high-sensitivity application fields, such as sensors, lasers, and storage of information with optical

devices.

Statements and Declarations

The authors declare that there are no conflicts of interest related to this article.

References

- [1] ORGHICI R, LÜTZOW P, BURGMEIER J, et al. A microring resonator sensor for sensitive detection of 1, 3, 5-trinitrotoluene (TNT)[J]. *Sensors*, 2010, 10(7): 6788-6795.
- [2] MI G, HORVATH C, VAN V. Silicon photonic dual-gas sensor for H₂ and CO₂ detection[J]. *Optics express*, 2017, 25(14): 16250-16259.
- [3] SHI S, CHENG Q, LIN R, et al. Micro-ring sensor used in the diagnosis of gastric cancer[C]//International Conference on Optoelectronics and Microelectronics Technology and Application, October 10-12, 2016, Shanghai, China. Washington: International Society for Optics and Photonics, 2016: 102441K.
- [4] FENG X, ZHANG G, CHIN L K, et al. Highly sensitive, label-free detection of 2, 4-dichlorop-henoxyacetic acid using an optofluidic chip[J]. *ACS sensors*, 2017, 2(7): 955-960.
- [5] CHANG C M, SOLGAARD O. Fano resonances in integrated silicon Bragg reflectors for sensing applications[J]. *Optics express*, 2013, 21(22): 27209-27218.
- [6] ZHU J, LOU J. High-sensitivity Fano resonance temperature sensor in MIM waveguides coupled with a polydimethylsiloxane-sealed semi-square ring resonator[J]. *Results in physics*, 2020, 18: 103183.
- [7] CHAUHAN D, ADHIKARI R, SAINI R K, et al. Subwavelength plasmonic liquid sensor using Fano resonance in a ring resonator structure[J]. *Optik*, 2020, 223: 165545.
- [8] QIU W, NDAO A, VILA V C, et al. Fano resonance-based highly sensitive, compact temperature sensor on thin film lithium niobate[J]. *Optics letters*, 2016, 41(6): 1106-1109.
- [9] ZHANG X, QI Y, ZHOU P, et al. Refractive index sensor based on fano resonances in plasmonic waveguide with dual side-coupled ring resonators[J]. *Photonic sensors*, 2018, 8(4): 367-374.
- [10] GU L, FANG L, FANG H, et al. Fano resonance lineshapes in a waveguide-microring structure enabled by an air-hole[J]. *APL photonics*, 2020, 5(1): 016108.
- [11] LU L, ZHU L, ZENG Z, et al. Fano resonance ion sensor enabled by 2D plasmonic sub-nanopores-material[J]. *IEEE sensors journal*, 2021, 21(13): 14776-14783.
- [12] HAUS H A, HUANG W. Coupled-mode theory[J]. *Proceedings of the IEEE*, 1991, 79(10): 1505-1518.
- [13] ZHANG C, KANG G, XIONG Y, et al. Photonic thermometer with a sub-millikelvin resolution and broad temperature range by waveguide-microring Fano resonance[J]. *Optics express*, 2020, 28(9): 12599-12608.
- [14] QIU C, HU T, YU P, et al. A temperature sensor based on silicon eye-like microring with sharp asymmetric Fano resonance[C]//The 9th International Conference on Group IV Photonics (GFP), August 29-31, 2012, San Diego, USA. New York: IEEE, 2012: 123-125.
- [15] ZHANG Y, ZOU J, HE J J. Temperature sensor with enhanced sensitivity based on silicon Mach-Zehnder interferometer with waveguide group index engineering[J]. *Optics express*, 2018, 26(20): 26057-26064.
- [16] DING Z, LIU P, CHEN J, et al. On-chip simultaneous sensing of humidity and temperature with a dual-polarization silicon microring resonator[J]. *Optics express*, 2019, 27(20): 28649-28659.
- [17] CHEN F, ZHANG H, SUN L, et al. Temperature tunable Fano resonance based on ring resonator side coupled with a MIM waveguide[J]. *Optics & laser technology*, 2019, 116: 293-299.
- [18] XU Y, OU Z, CHEN J, et al. High sensitivity refractive index and temperature sensors with tunable multiple Fano resonances[C]//2021 IEEE 6th Optoelectronics Global Conference (OGC), August 31-September 3, 2021, Shenzhen, China. New York: IEEE, 2021: 239-242.